ELSEVIER

International Journal of Mass Spectrometry 213 (2002) 9–24

International Journal of Mass Spectrometry

www.elsevier.com/locate/ijms

# Drift time mass spectrometric protein hydration experiments

J. Woenckhaus*

*Physical Chemistry I, Otto-Hahn-Str. 6, 44227 Dortmund, Germany*

Received 5 March 2001; accepted 17 July 2001

**Abstract**

Recent developments in electrospray ionization opened the field of mass spectrometry for macromolecules like proteins. The combination of ionization, drift time spectrometry, and mass spectrometry combines a large field of experimental techniques. In this new field it becomes possible to understand the interactions of isolated proteins with reaction partners like water. The combination of these techniques allows one to determine structural and thermodynamic properties. The experiments presented here give a first insight into the interaction of isolated protein ions with single solvent molecules. Results are presented for proteins like cytochrome C, bovine pancreatic trypsin inhibitor and lysozyme. MD-simulations on the same proteins and conditions as similar as possible to the experiments reflect the experimental results remarkable well. (Int J Mass Spectrom 213 (2002) 9–24) © 2002 Elsevier Science B.V.

*Keywords:* Ion mobility; Protein hydration; Electrospray ionization; Collision cross sections

## 1. Introduction

Water plays a fundamental role in life. All biological processes take place in an environment, which contains water. Focusing on proteins, any biological process involving proteins needs water to work. To be biochemically active a protein has to be in a special structure, the three-dimensional active structure. Water molecules stabilize this active structure. On the one hand the polar side chains of a protein are mostly facing to the surface of a protein in a polar solvent like water; on the other hand the polar side chains are facing mostly into the protein when the protein is in an unpolar solvent. The folding of a large variety of proteins is promoted with polar molecules like water. The process of protein folding is yet not fully resolved. Protein folding is the essential key in biological processes. Changes in the structure, often only a small change of the structure, is essential for its activity. Tremendous efforts have been undertaken to bring some insight to the process of protein folding. The hydration of proteins has been investigated with nearly all experimental methods like nuclear magnetic resonance (NMR) [1,2] circular dichorism [3], small angle x-ray scattering (SAXS) [4], small angle neutron scattering (SANS)[4], infrared spectroscopy [5] and mass spectrometry (MS) [6]. Parallel to the experimental approaches theoretical models have been developed and tested to give a further insight into protein folding. The necessity of a hydration shell for a protein was pointed out already in an article of Kuntz and Kauzmann in 1974 [7]. A protein crystal, where the structure is considered to be similar to the

* E-mail: woenckha@steak.chemie.uni-dortmund.de


*PII* S1387-3806(01)00504-8

structure in solution, consists of 25 to 90% of solvent [8]. However, there has been surprisingly little work on the hydration of biomolecules in the gas phase [9–11]. Klassen and collaborators [10] have measured free energy changes at 293 K for the fast steps in the hydration of some small peptides, the largest being $Gly_4H^+$. The Lee group has investigated hydrated peptides with Fourier transform ion cyclotron resonance mass spectrometry recently [12]. The investigated proteins are gramicidin S and bradikinin. It was found that the distribution of cluster sizes is very complex and exhibits magic numbers at 8, 11, 14, and 40 water molecules during solvent evaporation for the doubly protonated gramicidin S. The gramicidin S 40 water molecules cluster was assigned to a stabilized clathrate structure. For doubly protonated bradikinin no magic numbers for the water clusters were found which is in agreement that this molecule does not form stabilized clathrates.

The theoretical models of protein folding are getting more and more sophisticated as the computer power increases. Although the latest results are very promising, they do not yet provide the final key in understanding protein folding. Groups like Šali [13] and Dill [14] are developing models to bring insight into the folding process of proteins with computer simulations. Pioneers in unrevealing the problems of understanding the thermodynamics of hydration and protein folding are Makhatadze and Privalov [15,16].

NMR experiments to study proteins were performed already in the 1970's. Here the results increase with the growing resolving power of the spectrometers. The hydration of proteins is investigated in a large number of NMR experiments. It is possible to study the effect of one selected water molecules to a protein in aqueous or water/solvent containing solution [17,18]. With these methods, except mass spectrometry, it is impossible to investigate the effect of a single water molecule on a single protein molecule in the absence of solvent.

Circular dichroism is an often used tool to investigate protein folding in solution [3]. Here the same problem as in NMR spectroscopy arises: The effect of stepwise hydration of isolated proteins cannot be investigated due to the necessary presence of a large quantity of protein and solvent. SAXS and SANS are also methods to investigate the effect of hydration of proteins [4,19,20]. Using high pressure as a perbutation technique the kinetics of the unfolding can be studied with SAXS [21,22]. Infrared spectroscopy, like all other methods mentioned is incapable to allow the investigation of isolated proteins. On the other hand this method is one of the most often used to investigate structure, folding, and hydration of proteins in the bulk [5,23]. With these methods it is impossible to trace the question: What effect has a single water molecule on an isolated protein? Only mass spectrometry provides one with the possibility to investigate isolated protein ions and the reaction of isolated proteins with a defined amount of molecules of a reaction partner.

Mass spectrometric methods to investigate proteins in the gas phase have been set up when the ability of transferring proteins into vacuum was created. Mass spectrometry of protein ions is a relatively young experimental method. The mass spectrometry of intact biomolecules was limited to a mass range below $10^3$ u because of the difficulties of evaporating and transferring a protein molecule into the vacuum. The large biomolecules are fragmented during the process of evaporization or during the process of ionization. Mass spectrometry of large biomolecules was established with the introduction of two new evaporization and ionization techniques: matrix assisted laser desorption and ionization (MALDI) [24] and electrospray ionization (ESI) [25]. The advancement in these technologies allows the user of mass spectrometers to investigate biomolecules up to a mass of $10^8$ u [26]. The evaporization / ionization in these techniques are so gentle that it is possible to investigate van-der-Waals bound complexes. To study conformational aspects of gas-phase proteins, H/D exchange can be used [27–29]. Not only the exact mass is available with mass spectrometry, it is a versatile method to study structure, folding intermediates and especially due to the method it allows to study isolated proteins, reactions and noncovalent bindings between substrates and solvent molecules.

## 2. Experimental

Mass spectrometry and gas-phase reactions of proteins were impossible before MALDI and ESI were established since proteins have due to their high mass a nondetectable vapor pressure. The vapor pressure can be estimated and is about $10^{-475}$ Pa for a protein with a mass of 14 000 u at 25 °C [30]. Heating the protein sample to evaporate is in all cases not efficient. The sample rather decomposes than vaporize. MALDI and ESI are the solution to the problem. In 1987 the group of Karas [24,31] investigated the interaction processes of ultraviolet light with organic molecules and presented the first MALDI-MS experiments. In MALDI-MS the analyt is dissolved in a light adsorbing matrix in the molar ratio of 1:1 000 to 1:10 000 on a target. A short intense laser pulse evaporates the matrix together with the protein. The target with the mixture of protein/matrix is placed in an electric field. This allows when the laser light evaporates the matrix together with the protein sample, that the formed protein ions are extracted by the electric field. The protein ions are then focused into the mass spectrometer. Using the MALDI technique it is necessary to transfer the protein into a matrix. Here the possibilities to mimic a biological environment is very limited. In contrast, using the electrospray technique allows one to obtain the protein ions in various solution conditions that reflect different biological conditions, as different pH or polarity of the solvent.

ESI is even more versatile since the electrospray conditions can be tuned in a wide range giving the opportunity to investigate on the one hand naked proteins which undergo a hostile environment during the electrospray process and on the other hand it allows, especially the nanospray technique to apply very mild contions so that a partially solvated molecule is obtained or noncovalently bound substrates are linked to the investigated protein. The solution properties of the sample influences the obtained protein ions. The obtained molecules reflect properties they had before the ESI process took place [32]. Smith and the group of Przybylski and Glockner [33,34] recently published review articles about the mass spectrometry of biomacromolecules produced by ESI. Recent reviews focus on the electrospray process [35] and the ESI Fourier transform mass spectrometry [36,37].

The formation of naked protein ions in the electrospray process can be divided into two steps, the initial production of charged droplets and the subsequent ion formation process [38–40]. The droplets are formed at the tip of the electrospray needle and are dragged by an electric field between needle and vacuum interface. During ion formation the produced droplets shrink due to solvent evaporation. This can be assisted by a counterflow of dry nitrogen gas or by heating the ESI needle. The droplets shrink down to the level where repulsive coulombic forces approach the level of droplet cohesive forces (e.g. surface tension) further shrinkage stops. Two mechanisms are currently preferred for the ion formation from charged droplets: Direct field evaporation of the ion and droplet fission at the Rayleigh limit [41,42]. When the droplet is very small it becomes even smaller by a fission process that yields smaller and smaller droplets until the electric field at the droplet surface is sufficient for ion evaporization. Röllgen and coworkers [43,44] criticized the ion evaporization process pointing out that the actual field strength is not sufficient for ion evaporization. They suggest that the formation of ions are due to coulombic expulsion of smaller, less highly charged droplets. The ionization process is not revealed in detail. As suggested in the review of Smith and coworkers [39] the products of the two different ionization process may be indistinguishable. Using a drift cell with a reversible electrical field the ions spend a long time in the drift cell passing a Phase Doppler Anemometer gaining information about the evaporating and discharging of the droplet time dependent. The group of Smith uses an ion mobility spectrometer for these experiments. The experiments perfomed by the Smith group [45] proof that the evaporation process is a fission process at the Rayleigh limit. The amount of produced ions is small. About 10 to 100 pA of integrated ion current is produced. The ion current of the proteins is only a small fraction of it. In an injected ion drift tube instrument the signal of the ions leaving the drift tube is further reduced.

Another important improvement came about be-

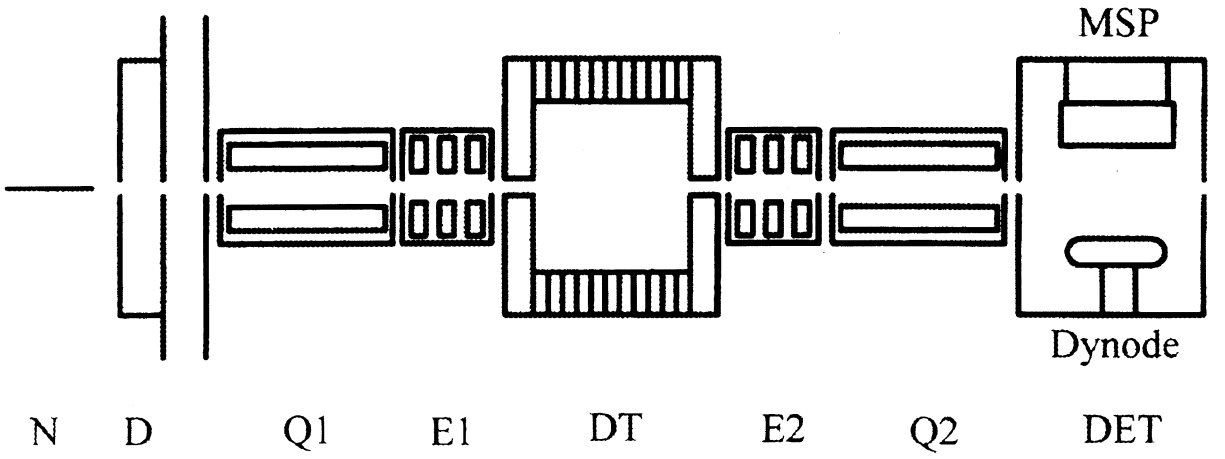


Fig. 1. Schematic view of the injected drift tube apparatus. From the left to right: needle (N) and desolvation region (D) of the electrospray source, first quadrupole (Q1) with electrostatic lenses (E1), drift tube (DT), electrostatic lenses (E2), second quadrupole (Q2), and detector (DET) with dynode and micro sphere plates (MSP).

tween 1960 and 1963 on the experimental side with the development of the drift-tube mass spectrometer [46]. Kaneko et al. developed the injected drift tube [47] in 1966. The combination of the new soft ionization techniques and the drift-tube mass spectrometer opened in 1995 a new field in mass spectrometry of large biomolecules. The groups of Helden using MALDI [48] and Clemmer using ESI [49], combined these soft ionization techniques with drift-tube mass spectrometers. The Dugourd group constructed a high resolution drift-tube mass spectrometer [50] in 1997 that has an increased resolution of a factor of 10 to a so-called low-resolution spectrometer. The drift tube of the group of Smith [45] has, like the drift tube of the Dugourd group [50], a direct interface to the ESI source. The group of Purves developed in 1998 an ion mobility spectrometer with a high frequency, high voltage electric field [51]. The group of Hoaglund uses a drift tube with an ion trap at the entrance to enhance the signal rate [52] to overcome the poor signal rates one obtains in the drift tube mass spectrometry.

Due to the experimental difficulties only the limited group of the above mentioned scientists use drift time techniques to study the conformation and reactivity of biomolecules and especially of proteins in the gas phase.

### *2.1. The drift tube apparatus*

The ESI source consists of a hypodermic needle that is kept at a potential of 5 kV with respect to ground. The protein solution is pumped with a syringe pump into the hypodermic needle. About 1 cm away from the tip of the needle the entrance orifice of the desolvation region is located. In Fig. 1 a schematic of a typical drift tube apparatus is shown. The entrance orifice is kept at a potential of several volts with respect to ground, the pressure is kept at around 10 Pa. The diameter of the entrance hole is about 200 $\mu$m. The protein ions enter through a small hole from the desolvation region into the first vacuum stage of the differential pumping system. Here the vacuum is maintained at less than $10^{-5}$ mbar. The ions pass through a quadrupole mass filter and the desired charge state of a naked protein can be selected. An appropriate electrical field injects the selected protein ions into the drift tube. The injection energy to the protein ions is determined by the electrical field between the entrance of ions into the vacuum and the entrance of the drift tube. If the singly charged ions enter the vacuum at an orifice that is kept at ground potential and the entrance of the drift tube is at $-100$ V, the ions have an injection energy of 100 eV. (cytochrome C + 7H)$^{+7}$ ions for instance

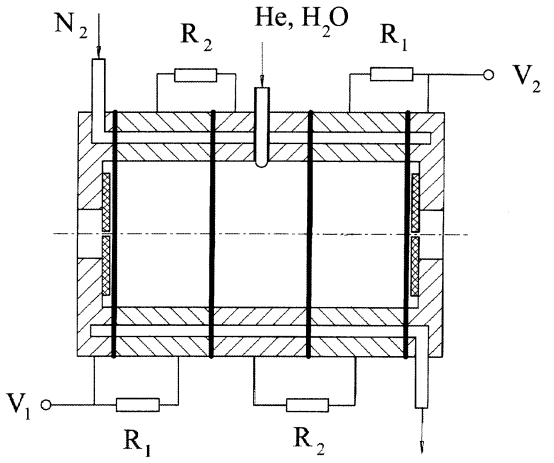


Fig. 2. Schematic drawing of the drift tube. The voltage difference between V1 and V2 determines the drift voltage. To obtain a uniform electrical field along the flight axis, a resistor chain is connected over the guard rings of the drift tube. The guard rings are insulated from each other by a kapton© foil. The heaters are not shown. The cooling is maintained with cold gaseous nitrogen, which is regulated and flows through several cooling tubes in the guard rings of the drift tube. The entrance and exit orifice have diameters of ~0.2 mm.

which pass after the electrospray source orifice to the entrance of the drift tube an electric field of 300 V have an injection energy of 2100 eV [53]. The drift tube is a gas filled tube with an entrance and exit orifice. In the drift tube there exists a uniform electrical field along the flight axis. A voltage gradient along guard rings generates the electrical field. Fig. 2 shows a drift tube schematics in more details. Leak valves and capacitance pressure gauges of the MKS-baratron type control the gas pressure in the drift tube. A way of adjusting the temperature of the drift tube is to control a nitrogen gas flow through a thermostable jacket and the use of electrical heaters. With this equipment the parameters of injection voltage, pressure, gas composition, temperature, and drift voltage can be easily controlled and varied. An electrical field that triggers the ions allows a short pulse of protein ions to enter the drift tube. The residence time in the drift tube is depending on the mobility of the ion. After passing the drift tube, the ions are mass analyzed with a second quadruole mass filter.

The drift time $t_d$, the time the ions spend in the drift tube, is related to the reduced mobility $K_0$,

$$K_0 = \frac{L}{t_d E}\frac{27{,}315}{T}\frac{P}{760}; \quad (1)$$

where $L$ is the length, $E$ the electrical field, $T$ the temperature, and $P$ the buffer-gas pressure. The drift time depends on the average collision cross sections [46]:

$$\Omega_{avg}^{(1,1)} = \frac{(18\pi)^{1/2}}{16}\left[\frac{1}{m}+\frac{1}{m_b}\right]^{1/2}\frac{ze}{(k_b T)K_0}\frac{1}{\rho} \quad (2)$$

Here $m$ is the mass of the ion, $m_b$ is the mass of the buffer gas, $ze$ is the charge of the ion, and $\rho$ is the buffer-gas density at STP.

The ions that enter the drift tube are decelerated by collisions with the buffer gas in the drift tube. The ions are shortly heated by the collisions and are finally thermalized at the temperature of the buffer gas. The heating of the ions is dependent on the injection energy. A gentle injection with a nonsignificant heating is achieved by lowering the injection energy as much as possible.

The hydration experiments were done by introducing a mixture of buffer gas and water vapor into the drift tube. For the mass selection in front and behind the drift tube, quadrupole mass filters with wide mass ranging from 5 to 4000 u are used. The ions travel in the whole experiment on an optical axis which allows adjusting all orifices with a light source visually.

The high-resolution solvent depended experiments were done in a drift tube that is constructed differently. The interface of the ESI source is connected directly to the drift tube. There is no differential pumping stage and quadrupole mass filter between the ESI source and the drift tube. The drift tube in this apparatus is kept at pressures between around 0.5 bar and the drift field is around 200 V/cm. Details of this apparatus are described [32].

### 2.2. The proteins used in the experiments

Hen egg white lysozyme is a very compact protein with a complex fold. It is a small protein with 14.6

kD. Lysozyme has a single peptide chain with 129 residues. The protein has four cross-linked disulfide bridges and is very stable. The interior of lysozyme is almost entirely nonpolar. Bovine pancreatic trypsin inhibitor (BPTI) is also a very compact protein. BPTI inhibits trypsin by binding to its active site. It is a 6 kD protein with 58 residues. Three disulfide bridges stabilize the protein. The two other proteins used for the major investigations are cytochrome C and myoglobin. Cytochrome C is present in all organisms having mitochondrial respiratory chains. This electron carrier evolved more than 1.5 billion years ago. Cytochrome C is a protein with 104 residues and a molar weight of 12.3 kD. The protein has a heme group and has no disulfide bonds. Myglobin is a protein that has a heme group too. The protein plays an important role in the oxygen transport in muscles. The protein consists of 153 residues. Myoglobin is built primarily of eight $\alpha$ helices, the remaining are turns between the alpha helices. The molar weight of the very compact protein is 18 kD. It has no disulfide bonds and the interior of the native form of the protein is highly unpolar. The selected proteins can be divided into two groups that can be assigned as follows: Disulfide bridge and rigid and into nondisulfide bridge containing nonrigid proteins. The crystal structures of all these proteins are well known [54–57].

### *2.3. The experiments*

#### *2.3.1. Proteins: Structure and folding under the influence of hydration*

Shelimov and Jarrold found that the cross section of unsolvated cytochrome C depends on the charge state and the injection energy. The cross section varies with the ionization state and injection energy of the protein [58] (Fig. 3). The electrical field determines the injection energy the ions pass prior entering the drift tube and the charge state. The charge states of the investigated proteins M are $(M+nH)^{+n}$, not always in the text are the hydrogen ions mentioned.

In 1996 Shelimov and Jarrold discovered that cytochrome C which in solution is denaturated and unfolded, refolds in the desolvation region to a compact structure which is comparable to the crystal

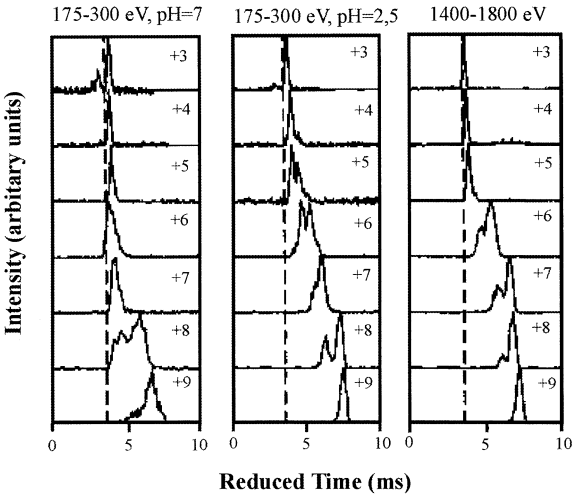


Fig. 3. Drift time distribution recorded for the +3 to the +9 charge states of cytochrome C. The first column was recorded with low injections energies varying from 175 to 300 eV. The solution was kept at a pH = 7. The column in the middle was recorded from a solution with a low injection energy from 175 to 300 eV and a pH = 2.5. At low injection energies the drift time is dependent on the charge state and pH of the electrosprayed solution. The column at the left was recorded with high-injection energies from 1400 to 1800 eV. Here the drift time is only dependent on the charge state. The drift time distributions are plotted against a reduced time scale by multiplying the measured drift times by the charge (+3 up to +9). The dotted vertical lines show the drift time one obtains by calculating the drift time from the crystal structure with the trajectory model [62].

structure when a strong base(1,3,4,6,7,8-hexahydro-l-methy-2h-pyrimido [1,2-a] pyrimidine) is added into the desolvation region [59]. The strong base strips off protons from the higher charged ions and thus lower charged ions are formed. These experiments were undertaken conceptually similar to experiments from Gross [60] and Wood[61]. Gross et al. [60] reported indirect evidence, from gas-phase basicity measurements, for the folding of lysozyme following charge stripping. Wood et al. [61] have employed H/D exchange to examine the conformations generated by proton stripping to the +7 charge state of cytochrome C and found a substantial reduction in the number of exchangeable hydrogens. In contrast to this Shelimov and coworkers [59] found that it is possible to generate the +7 charge state in a conformation almost as compact as the native conformation by electrospraying a not acidified, neutral, solution. They

showed that the +7 charge state of cytochrome C, which undergoes proton stripping in the desolvation region, refolds to a conformation that is more compact than the native structure derived from x-ray crystallography [59]. The calculation of the cross section is possible when the structure is known. This calculation is performed using the trajectory model from Mesleh and coworkers [62].

Hudgins and coworkers modified a high-resolution drift tube apparatus designed for cluster research as an electrospray drift time mass spectrometer at Evanston in 1997. In 1998 the group of Wu presented a similar experimental setup [63]. The measurements show that not only the charge states of the protein in the gas phase influence the structure. The proteins that were electrosprayed in the high-resolution drift tube instrument are ionized and injected under much gentler conditions than in the drift tube apparatus. Hudgins et al. showed that the structure of the electrosprayed proteins is also depending on the solvent [32]. It is for instance possible to distinguish between (cytochrome C + 8H)$^{+8}$ ion electrosprayed from an aqueous solution, a 1:1 water/methanol solution, and an acidified (6% acetic acid in a 1:1 water/methanol solution) solution. See details in Fig. 4. Higher charged cytochrome C like the +12 to +14 charge state show a dependence on acid concentration (Fig. 5), they unfold further as the acid concentration rises. These measurements were possible because no injection energy is involved in the high-resolution drift tube experiments and so soft introduction of protein ions into the drift tube is realized. The results are an indication that the formation of the ions in the electrospray process follow the proposed path of Röllgen and coworkers [43,44], if it would follow the path as predicted by Thomson [41] the information that arises from the solution would be lost in the gas phase. Furthermore, it is to mention that the group of Smith realized experiments [45] that prove the pathway proposed by Röllgen. Iavarone and coworkers investigated the solvent influence on the formed protein ion *m/z* ratio recently [64]. The high-resolution drift tube mass spectrometers have not been used to investigate hydration of proteins jet.

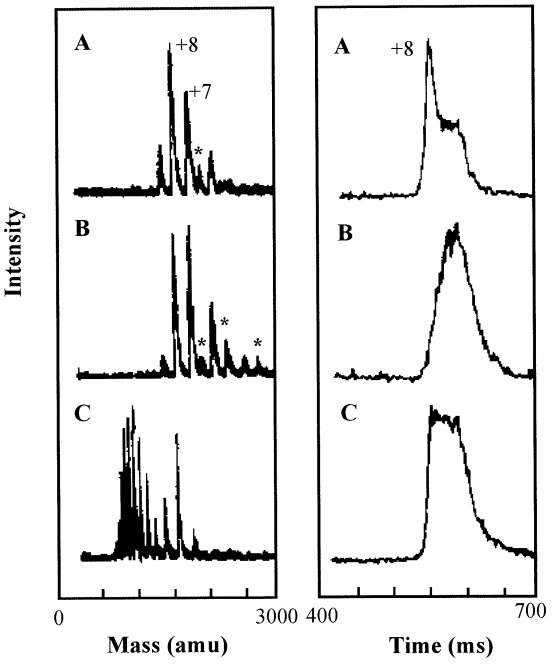


Fig. 4. Mass spectra (left) and drift time distributions (right) for the +8 charge states of bovine cytochrome C measured with the high resolution instrument using different solutions. The three solutions employed were: an unacidified aqueous solution (A), an unacidified 1:1 water and methanol solution (B), and a 3:1 water acetonitrile solution with 6% acetic acid (C). The drift times here are reduced drift times, which are obtained by multiplying the drift times by the charge.

### *2.3.2. Temperature experiments on nonhydrated cytochrome*

As mentioned in the experimental section, the temperature of the drift tube can be adjusted. Mao and coworkers used this feature to investigate the thermal unfolding of cytochrome C in the gas phase [65]. The (cytochrome C + 5H)$^{+5}$ charge state is surprisingly resistant against collisional and thermal heating. During collisional heating no substantial change in the cross section is observed. Also during thermal heating in a temperature range from 273 to 571 K the +5 charge state of cytochrome C undergoes no substantial changes. Unlike the +5 charge state of cytochrome C the +6 and +7 charge states depend strongly on the injection energy and temperature in the drift tube. At low injection energy cytochrome C retains a memory of the structure in solution and

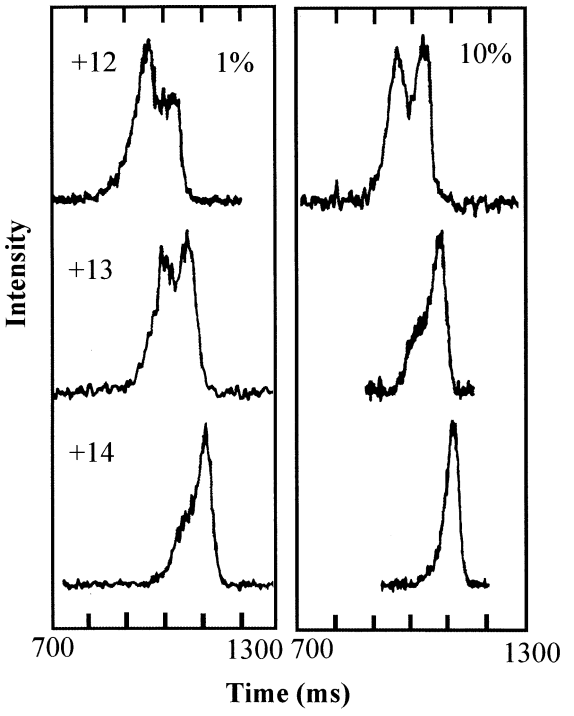


Fig. 5. Drift-time distributions recorded for the +12 to +14 charge states of bovine Cytochrome C with solutions of 3:1 water and acetonitrile with 1% (left) and 10% (right) acetic acid. The reduced drift time is obtained by multiplying the drift time with the charge.

shows a conformation that is comparable to the crystalline structure [32]. At high injection energies the ions are due to the collisions with the exiting buffer-gas first heated while entering the drift tube and then inside of the drift tube they are thermalized. The cross section of cytochrome C in the charge state +7 varies with the temperature as shown in Fig. 6 for low and high injection energies. The cross section of the +7 charge state of cytochrome C, which is injected with low injection energies, undergoes several changes and shifts to larger cross sections when the temperature is increased. At 423 K a distribution with three peaks is present, which means three conformers are apparent under these conditions. When this charge state is injected with high injection energies we find two peaks in the cross section distribution at room temperature and at 423 K only one conformation is apparent. This peak overlaps with the 3rd peak that was obtained in the experiment with low

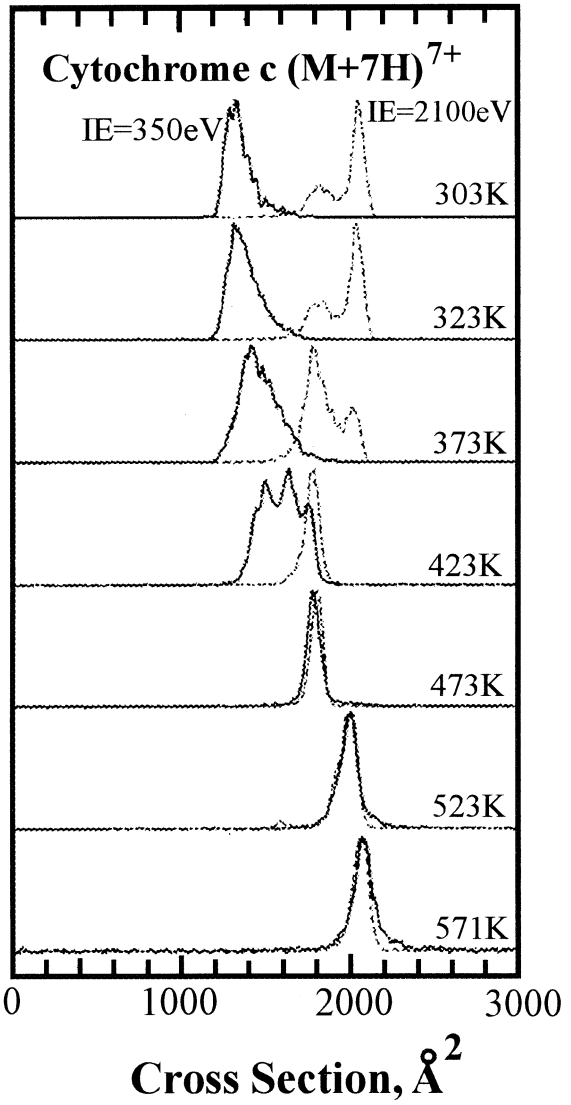


Fig. 6. Cross-section distribution measured for the +7 charge state of equine Cytochrome C as a function of distributions measured with low injection energy (350 eV), whereas the dashed lines show results obtained with high injection energy (2100 eV). The near vertical dashed line is a least squares fit to the collision integrals, calculated form the crystal structure as a function of temperature using the trajectory model [62].

injection energies. At higher temperatures (473 K) the cytochrome C + 7 charge state shows in the drift time spectra only one peak for the low and the high injection energy. Both peaks represent a similar cross section. When the temperature in the drift tube is

further increased, the peak shifts to higher cross sections, e.g. the protein unfolds further. One can conclude that at temperatures above 473 K the conformation is only depending on the temperature, the cross section becomes independent of the injection energy. In contrast to these results, the protein, BPTI shows for the charge states from +4 to +7 no dependence on temperature from about 250 to 650 K. This can be explained by the rigidity of the protein BPTI. BPTI has three disulfide bonds that stabilize the protein. The group of Valentine [66] has investigated folding of disulfide intact and reduced lysozyme in the gas phase in 1997; conformations and pathways of folding and unfolding are proposed. The disulfide intact lysozyme favors two types of conformers: a highly folded conformer with a cross section near to the calculated one for the crystalline structure and a partially unfolded conformer which is formed when the ions are injected into the drift tube at high injection voltages. The ions of the disulfide reduced lysozyme solution show in the gas phase a much larger collision cross section than the disulfide intact protein. These ions are in large sections unfolded. The disulfide reduced lysozyme ions favor low charge states in gas-phase proton transfer reactions. When these charge states fold up several new conformations comparable to those measured for the disulfide intact conformations are found. Arrays of misfolded, metastable, or folding intermediates can be detected.

### 2.3.3. Hydration of proteins

*Thermal properties of the cytochrome C hydration.* The present author and coworkers [67] measured the thermodynamic properties of the hydration of the first water molecules to cytochrome C charge states +5 and +7. Water vapor is mixed with the buffer gas of the drift tube. For the +5 and the +7 charge states of cytochrome C in the gas phase the free energy changes in the first steps of hydratation were determined from equilibrium constant measurements at 721 K. Ion mobility measurements of the +5 charge state and the +7 charge state indicate that the +5 is folded while the +7 charge state is partially unfolded [58] under the employed conditions. Free energy changes for the adsorption of the first nine water molecules on the folded +5 charge state and the first five water molecules on the partially unfolded +7 charge state have been determined. For the transfer of water molecules from the bulk to the hydration shell of the protein the change in free energy is remarkably small, between −2 and −7 kJ $mol^{-1}$. This indicates a very effective shielding of charge in both the unfolded and folded conformation. For initial hydration of the folded +5 charge state of cytochrome C the free energy changes are significantly more negative than for the unfolded +7 state. This indicates that the charge is more effectively shielded in unfolded +7 charge state, or may be the incorporation of some of the adsorbed water molecules as structural water in the folded +5 charge state. One possible interpretation of this behavior could be given by the presumption that the water molecules entered the folded +5 charge state as structural water molecules. Only six structural water molecules have been found for cytochrome C in recent NMR studies [68]. The experiments where compared with measurements from Klassen [10] et al. on $GlyH^+$ (Fig. 7) and the adsorption of water molecules on $H_3O^+$ [69].

*Structural changes of proteins upon hydration of cytochrome C and apomyoglobin.* Fye and coworkers [70] investigated the structural changes of cytochrome C upon hydration in the gas phase. The average numbers of water molecules adsorbed on this protein is depending on the charge state and structure of the protein. The amount of water molecules is larger for the compact and folded low charge states than for the unfolded higher charge states. The +5 charge state adsorbs about 50 water molecules. This number decreases to around 25 water molecules on the $(M + 9H)^{+9}$ ion and with further increasing charge on the protein it gradually increases again. There is a strong correlation between the sharp decrease in the number of adsorbed molecules and the unfolding transition evident in the cross section measurements, as shown in Fig. 8. It was found that the free energy changes at 273 K for the adsorption of the first few water molecules on the folded +5 charge state of cytochrome C to be larger than on the unfolded +7 charge

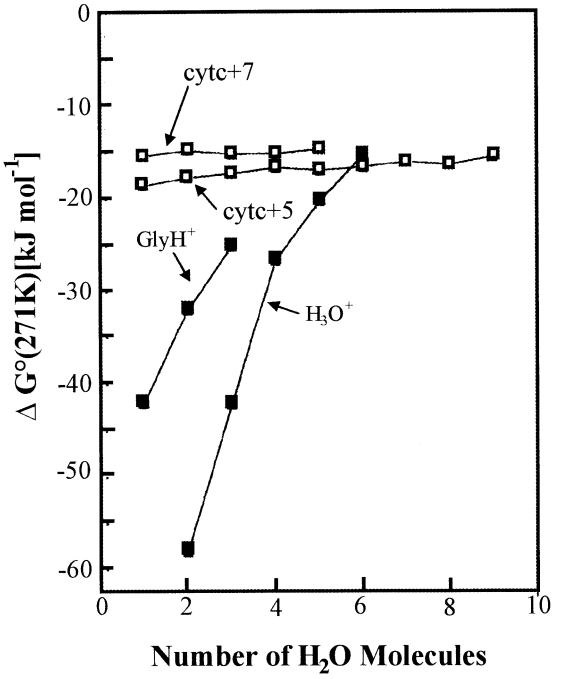


Fig. 7. Free energy changes ΔG° for the adsorption of a water molecule onto the +5 and the +7 charge states of cytochrome C plotted against the number of adsorbed water molecules. Free energy changes for the adsorption of water onto $H_3O^+$ [69] and $GlyH^+$ [10] are shown for comparison.

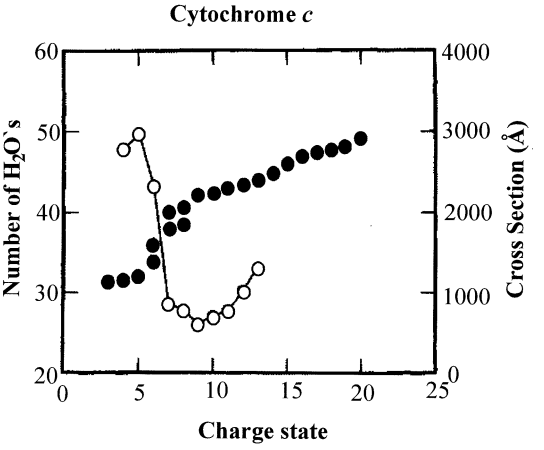


Fig. 8. Plot of the average number of water molecules adsorbed on cytochrome C ions with 97.3 Pa of water vapor at −20°C (open circles and left hand scale). The average cross sections, determined from ion mobility measurements [58] are also shown (full circles and right hand scale).

state [67]. The low free energy changes found in the studies of the first few steps in the hydration of cytochrome C indicate that the charge is effectively self solvated. However, an increase in the charge should result in an increase in the number of adsorbed water molecules A systematic increase in the average number of adsorbed water molecules is seen for cytochrome C + n ions with n > 9. Compared to cytochrome C, apomyglobin is around 50% larger and the unfolding transition is broader and shifted to higher charge states. The +5 and +6 charge states are able to adsorb around 60 water molecules in average. This number decreases down to 25 water molecules on the $M^{+10}$ ion for apomyglobin ion and with increasing charge on the protein it gradually increases again (not shown here). This increase in both proteins probably results directly from the increased charge and indirectly from the charge causing the protein to unfold further and expose more-favorable hydration sites. Solvation energies of proteins are usually estimated from an accessible surface area (ASA) model where the solvation energy is given by [71,72]

$$\Delta G_{solv} = \sum_i ASA_i C_i \quad (3)$$

In this expression $ASA_i$ is the accessible surface area for group *i*. $C_i$ is a coefficient determined by fitting solvation data for model compounds. There is evidence that this group additivity approach fails for molecules with several polar groups. For example, the free energy changes for transferring p-hydroxylbenzyl alcohol and m-hydroxybenzyl alcohol between toluene and water differ by 13.2 kJ $mol^{-1}$. This large difference has been attributed to the two hydroxyl groups in m-hydroxybenzyl alcohol being at almost an ideal distance to form a hydrogen-bonded chain with a water molecule [73]. There is a striking contradiction between the expected results from ASA approximation and the fact that the number of adsorbed water molecules at the unfolded state of cytochrome C and apomyoglobin is substantially smaller than for the folded charge states. This indicates that cooperative effects play a role that cannot be neglected. It seems that water molecules strongly interact with more than one site at the protein, which

is very important for the hydration of the folded conformation. These results further indicate that solvation energy differences between unfolded and native conformations of proteins are overestimated by the ASA approximation, as suggested by the recent theoretical analysis of Lazaridis et al. [74]. These types of cooperative effects have been observed in the binding of $H_3O^+$ to polyethers in the gas phase [75,76]. In the gas phase the unfolding transition occurs between the +5 and the +7 charge states of cytochrome C, while in solution charge states $n^+$ up to around +11 remain folded [77]. The unfolding of the gas-phase proteins seems to be driven by Coulomb repulsions. This different behavior compared to the in water dissolved proteins is at least partly caused by the high dielectric constant of water. So, if water molecules are added to the unfolded +7 charge state in the gas phase, at some point the folding to a conformation similar to the native one should appear. Fig. 9 shows drift time distributions recorded for the folded +5 charge state and the unfolded +7 charge states of cytochrome C as a function of water vapor pressure. In these measurements a helium plus water vapor atmosphere of around 670 Pa is used. Because of the varying water vapor pressure the drift time scales had to be corrected [46] and were multiplied by the charge to remove its effect on the drift time resulting in a reduced drift time. The peak in Fig. 9 for the folded +5 charge state is found around 9 ms, which is close to the drift time expected and calculated for the native conformation. The peak does not shift with increasing number of adsorbed water molecules. The unfolded +7 charge state shows two peaks in the drift time distribution in the absence of the water, and with increasing number of adsorbed water molecules the distribution shifts over to the more folded conformation at shorter time. This observed behavior is explained with the folding of the +7 charge state to a more compact conformation by the addition of only 29 water molecules. However, to drive the +7 charge state to a completely folded conformation, which would be expected at 9 ms in fig 10, much more than 29 water molecules are needed. Similar water-induced folding transitions have been observed for the +7 charge state of apomyoglobin

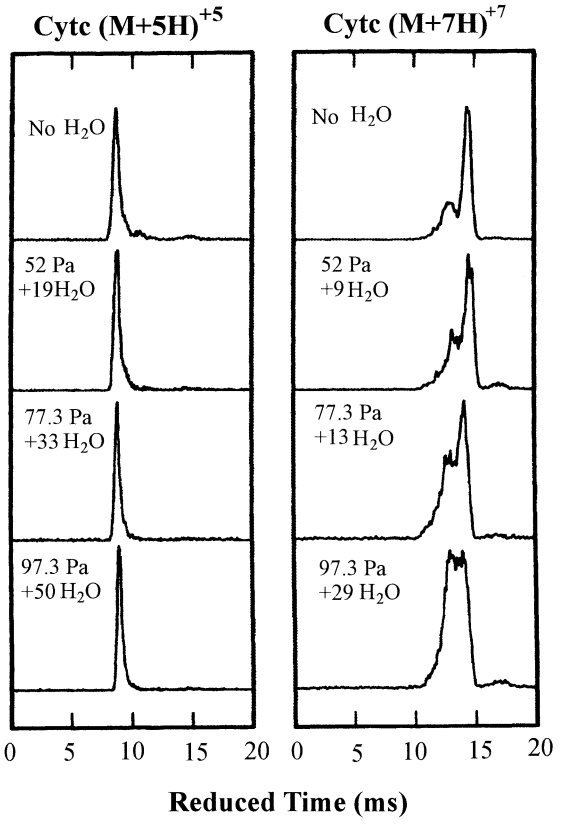


Fig. 9. Drift time distributions measured for the $(M + 5H)^{+5}$ and $(M + 7H)^{+7}$ charge states of cytochrome C with 0.0, 52, 77.3, and 97.3 Pa of water vapor. The water vapor plus helium buffer gas was around 666.6 Pa, and the drift tube was at −20 °C. The average number of adsorbed water molecules is shown for the different water vapour pressures for both charge states. The drift-time scale has been approximately corrected using Blanc's Law [46] to account for the different water vapor pressures, and the time scale has been multiplied by the charge to remove its effect on the drift time.

which emphases that the folding of a protein is promoted by the presence of water.

### *2.3.4. Hydration of bovine pacreatic trypsin inhibitor (BPTI)*

*Thermodynamic properties.* The initial step of the hydration of BPTI has been investigated [78]. BPTI is well suited for these studies because it is a small, extensively characterized protein. It has 58 residues and the backbone is partially locked by three disulfide

bridges. This makes BPTI very resistant to denaturation. Molecular dynamics simulations performed for BPTI in vacuum [79,80] suggest that the time-averaged structure is similar, but not identical to the crystal structure. The measurements of the enthalpy and entropy of the hydration of BPTI with single water molecules expose interesting results. The reaction $(BPTI + 6H)^{+6}(H_20)_n + H_2O = (BPTI + 6H)^{+6}(H_2O)_{n+1}$ was observed. A solution of $5 \times 10^{-5}$ M BPTI in a 50:50 mixture of water and methanol was electrosprayed at 5 kV in air. Electrospraying disulfide-intact BPTI gives mainly the +5 to +7 charge states. The charge distribution results from the protonation. The +6 charge state was selected and injected with an energy of 1200 eV into the drift tube. Inside the drift tube an electric field of 13.2 V $cm^{-1}$ and a total pressure of water vapor and helium of around 670 Pa is tuned in. The water vapor was raised from 0.2 to 32 Pa and the temperature of the drift tube was varied between 223 and 273 K. The ions spend 1 to 2 ms traveling through the drift tube. Then the ions are mass analyzed.

The obtained results reveal the presence of a special hydration site of gas-phase BPTI. It can be assumed that this site could be related to a unique structural water molecule, which is found for this protein in solution [17]. Previous information about thermodynamic properties and the interaction of water with proteins has been obtained from studies of the hydration of protein films [7,81]. Fig. 10 shows a mass spectrum recorded for the +6 charge state of BPTI. The conditions in the drift tube are 243.4 K and a water vapor pressure of 0.64 Pa. The unsolvated +6 charge state gives a signal at 1085 u, and peaks due to the addition of up to four water molecules are present. The line in Fig. 10 is a leasts squares fit to the experimental data using gaussian functions. Equilibrium constants for the hydration reactions were derived from

$$K = \frac{I[(BPTI + 6H)^{+6}(H_2O)_{n+1}]}{I[(BPTI + 6H)^{+6}(H_2O)_n P[H_2O]]} \quad (4)$$

where $P[H_20]$ is the water vapor pressure in atmospheres, $I[BPTI + 6H)^{+6}(H_2O)_{n+1}]$, and $I[(BPTI + 6H)^{+6}(H_20_n)]$ are the intensities from the fits in the mass spectra. Analog measurements were performed with a drift field half as strong as described above. The ions then spend a time twice as long in the drift tube. The results from these measurements with different drift times did not show differences, which gives evidence that the equilibrium is well established. However, the equilibrium constants show a small decrease with increasing water vapor pressure, which is not dependent on the drift field. This nonideal behavior can be explained by the presence of several closely related conformations with slightly different hydration properties. Ion mobility measurements for the +6 charge state of BPTI give results, which are close to those predicted for the native conformation [58]. However, the peak is slightly broader than expected for a single conformation, which indicates that more than one conformation is present. Crystal structure investigations show three slightly different structures for BPTI and the dispersion in the cross sections for these structures is comparable to the distribution observed in the ion mobility measurements [58].

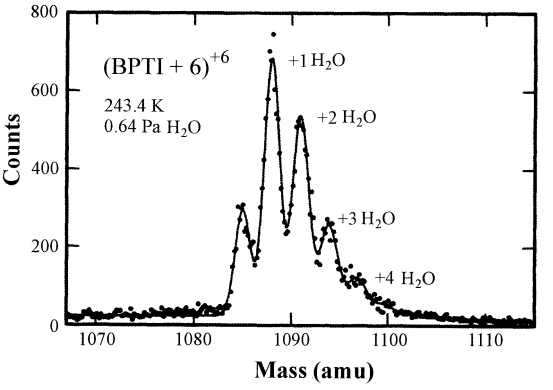


Fig. 10. Mass spectra of $(BPTI+6H)^{+6}$ at 243.15 K with 666.6 Pa He in the drift tube and 0.64 Pa water vapor. The line is a least-squares fit using Gaussian functions and the dots are the measured data. Peaks due to the addition of up to four water molecules are present.

Fig. 11 shows a plot of In $K$ against 1/T for the first six water molecules adsorbed by $(BPTI + 6H)^{+6}$. The slope of the lines gives $\Delta H°/R$, and the intercept gives $\Delta S°/R$. Fig. 12 shows $\Delta H°$ and $\Delta S°$ plotted versus the number of adsorbed water molecules. The

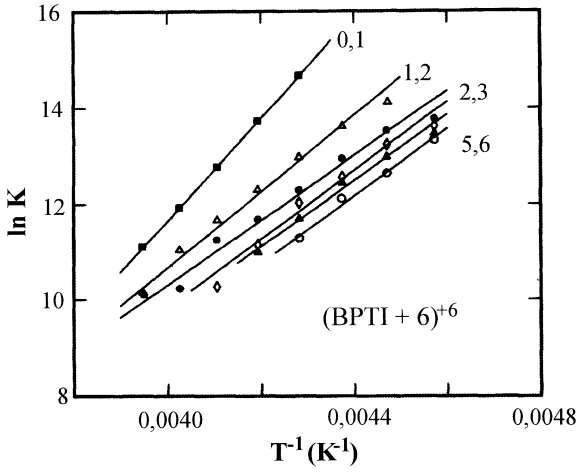


Fig. 11. Plot of K against 1/T for the addition of the first six water molecules to $(BPTI+6H)^{+6}$. For details see the text.

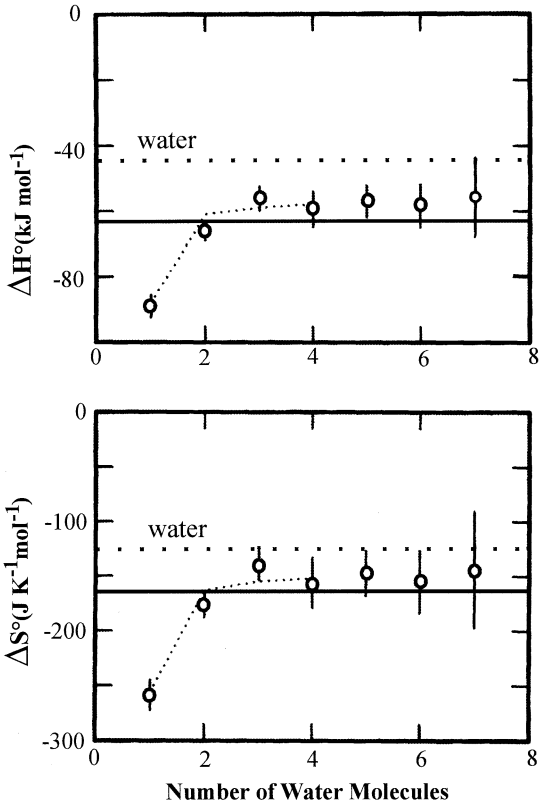


Fig. 12. Plot of the entropy and enthalpy changes for the adsorption of the first six water molecules onto $(BPTI+6H)^{+6}$. The dashed line represents the entropy and enthalpy changes for transferring a water molecule from the gas phase to liquid water. The horizontal lines show average values for $\Delta S°$ and $\Delta H°$ for the initial stage in the hydration of protein films.

error bars represent two standard deviations from the linear regression plus the estimated uncertainty associated with the slight pressure dependence of the equilibrium constants. $\Delta H°$ for the addition of the first water molecule is $-90 \pm 4$ kJ mol$^{-1}$. For subsequent water molecules, the enthalpy change is significantly less negative. The entropy changes follow a similar trend. $\Delta S°$ for the addition of the first water molecule is $-260 \pm 20$ J K$^{-1}$ mol$^{-1}$. The entropy and enthalpy change has been determined for up to the sixth adsorbed water molecules. However, equilibrium constants for the fourth to sixth water molecules have only been measured over a relatively narrow temperature range so that the values derived for $\Delta H°$ and $\Delta S°$ have a large uncertainty associated with them. The dashed lines show average values for $\Delta H°$ and $\Delta S°$ determined for the initial stage in the hydration of protein films, $\Delta H° = -60$ kJ mol$^{-1}$ and $\Delta S° \approx -160$ J K$^{-1}$ mol$^{-1}$. $\Delta H°$ and $\Delta S°$ for the second and subsequent water molecules adsorbed on $BPTI^{+6}$ are close to these values.

The entropy change for hydration is caused by the loss of the translational and rotational entropy of the water molecule and the increase in the vibrational entropy of the product. The translational and rotational entropies can be calculated. Using vibrational entropies deduced for water adsorption on ice and for the first few steps in the hydration of $H_30^+$ [69], an entropy change of $-100$ to $-140$ J K$^{-1}$ mol$^{-1}$ should be expected for the hydration reactions. The entropy change observed for the first water molecule is clearly much more negative than predicted. This indicates that the entropy of the protein must decrease by 100 to 120 J K$^{-1}$ mol$^{-1}$ when the first water molecule is adsorbed. This entropy must be derived from the remaining configurational entropy of the protein BPTI. The large loss of configurational entropy probably results from the water molecule locking two parts of the peptide chain together. This behavior can occur with structural water molecules. Four structural water molecules have been identified for BPTI and these are conserved in all three crystal structures [82–84] and

have been observed by NMR in solution [85] too. One of the structural water molecules is hydrogen bonded in a pocket to Cys38, Cys14, and Thr11, the other three form a hydrogen-bonded cluster of water molecules that are hydrogen bonded to Pro8, Tyr10, Asn43, Lys41, and Asn44. The isolated structural water molecule is unusual in that it forms four hydrogen bonds to the protein. Calculations suggest that this is the most strongly bound hydration site of BPTI [86], with hydration energy of about 100 kJ $mol^{-1}$. Thus this is a reasonable candidate for the site of the first water molecule adsorbed in the gas phase. One concern with this assignment is that Cys14 and Cys38 are already linked by a disulfide bridge, so it is not obvious that binding a water molecule in this site should lead to such a large entropy change. However, the hydrogen bond to Thr11 will constrain the protein, and Thr11 is in turn hydrogen bonded to Gly36, so introducing the water may cause the whole pocket to order. The configurational entropy of an unfolded protein is large, roughly 3000 $J\,K^{-1}\,mol^{-1}$ for BPTI in vacuum [72]. So it is reasonable that a small fraction of the configurational entropy persists in the folded gas-phase protein and that this entropy is lost when water molecules adsorb and order the structure. The adsorbed water may also favor one of the many possible ways of arranging the protons among the basis sites, and this would also contribute to the lowering of the configurational entropy. The large enthalpy change observed for the first water molecule adsorbed could also be explained by this water solvating one of the charge sites. However, the charge sites are expected to be shielded by carbonyl oxygens, and charge solvation could not account for the remarkably large entropy change observed for the first water molecule adsorbed.

### *2.4. The computer simulation of the experiments*

The computer simulations of the presented experiments have been performed with MD simulations on the charge induced unfolding / refolding of cytochrome C, the thermal behavior of cytochrome C and on the hydration of BPTI. Mao and coworkers [87] have performed MD-simulations on the charged induced un- and refolding of unsolvated cytochrome C. For these simulations the Kolafa [88] molecular modeling package with CHARMM-like potentials [89] was used. The Coulomb potential was not truncated because this is unnecessary for the isolated protein ions studied. The bond lengths were constrained by SHAKE [90]. The simulations were performed for protonated uneven charge states between +3 and +19 of cytochrome C. In vacuo, ion mobility measurements show that cytochrome C ions unfold as the charge increases. Cross sections derived from the MD simulations are compared with the measured cross sections. The experimental results depend on the conditions employed. Cross sections derived from the MD simulations show the same trend in unfolding as the experimental data. The unfolding in the simulations occurs at a charge state of +11; the experiment shows the unfolding effect, depending on the conditions already at a charge state of +7. The cross section derived from the simulation is smaller than that found experimentally. The simulation comes to a closer agreement for higher charge states. When 10 protons are removed from the +19 charge state of cytochrome C, the resulting +9 collapses slightly by forming random loops. Mao and coworkers [65] have performed MD simulations on thermal unfolding of the +5 and +7 charge state of cytochrome C. Simulating the +5 charge state of cytochrome C in the temperature range from room temperature to 600 K reveals cross sections in the range from 1385 to 1451 $Å^2$. This is in good agreement with the experimental results of 1200 $Å^2$ at room temperature to around 1300 $Å^2$ at 571 K. The +7 charge state of cytochrome C shows a cross section of 1300 $Å^2$ at room temperature and increases to 2065 $Å^2$ at 571 K. The unfolding can bee seen in the MD simulation but depending on the starting point cross sections between 1500 to 2100 $Å^2$ are found. The MD simulation reproduces the experiment qualitatively. Three groups have investigated with MD simulation of the hydration of BPTI. Mao and coworkers [91] found the thermodynamical properties reproduced by the MD simulation. The simulation shows a value for the hydration of the water site W122 of $\Delta S° = 232$ $J\,K^{-1}\,mol^{-1}$. The experimental value is 260

$J\,K^{-1}\,mol^{-1}$. In this simulation a second site for the first water molecule was found. The water molecule at this site, Thr11, Arg20, Phe33, Asn44, is tetrahedrically coordinated as in the site, W122. It was further calculated that the proteins stiffen when a single water molecule is incorporated. In contrast to this Fischer and coworkers [92] found that simulating the water uptake of BPTI the vibrational frequencies in the range of 200 to 800 $cm^{-1}$ increases leading to an increase of flexibility of the protein structure. The group of Helms also investigated the properties of the hydration of BPTI. They used grand canonical Monte Carlo simulations. The results agree well with the experimental results allowing successfully modeling the dynamics of the tightly coordinated internal water molecules [93].

## 3. Conclusion

The experiments presented and MD simulations provide a closer insight into the interactions of isolated protein ions with solvents. The combination of electrospray, drift time spectroscopy, mass spectroscopy, and MD simulations opens up a wide field of experimental and theoretical approaches to the understanding of protein folding. The presented experimental technique enables one to examine isolated proteins and with the stepwise addition of solvent up to several hundred solvent molecule the interaction of protein ions with the solvent. It now becomes possible to approach information about intrinsic intramolecular and intermolecular interactions that cannot be obtained directly from solution studies. The experiments are on a molecular scale that makes MD simulations feasible. Due to the limited amount of participating molecules the MD simulation gives reasonable results in reasonable computing time. In the future the field of protein interactions will be opened to the interactions of proteins with substrates, protein–protein interactions, and noncovalently bound complexes. With the prospect of performing more sophisticated experiments and simulations this is an exciting research field.

## References

[1] K. Wüthrich, Acta Crystallogr. Sect. D. Biol. Crystallogr. 51 (1995) 249.
[2] K.T. Dayie, G. Wagner, Annu. Rev. Phys. Chem. 47 (1996) 243.
[3] N.J. Greenfield, Trends Anal. Chem. 18 (1999) 236.
[4] Hydration Processes in Biology: Theoretical and Experimental Approaches, M-C. Bellisent-Funel, (Ed.) IOS Press; Amsterdam; Washington, D.C. 1999. (Series: NATO Sci. Ser. A, Life sciences; Vol. 305)
[5] M. Jackson, H.H. Mantsch, Crit. Rev. Biochem. Mol. Biol. 30 (1995) 95.
[6] Biological Mass Spectrometry: Present and Future, T. Matsuo, R.M. Caprioli, M. L. Gross, Y. Seyama, (Eds.) Wiley & Sons, New York, 1995.
[7] I.D. Kuntz, W. Kauzmann, Adv. Protein Chem. 28 (1974) 239.
[8] T.E. Creigton. Proteins: Structure and Molecular Properties, 2nd ed.; Freeman, New York, 1993.
[9] S.K. Chowdhury, V. Katta, B.T. Chait, Rapid Commun. Mass Spectrom. 4 (1990) 81.
[10] J.S. Klassen, A.T. Blades, P.J. Kebarle, J. Phys. Chem. Soc. 99 (1995) 15509.
[11] S.E. Rodriguez-Cruz, J.E. Klassen, E.R. Williams, J. Am. Soc. Mass Spectrom. 8 (1997) 566.
[12] S.-W. Lee, P. Freivogel, T. Schindler, J.L. Beauchamp, J. Am. Chem. Soc. 120 (1998) 11758.
[13] A. šali, E. Shakhnovich, M. Karplus, Nature, 369 (1994) 248.
[14] K.A. Dill, H.S. Chan, Nat. Struct. Biol. 4 (1997) 10.
[15] G.I. Makhatadze, P.L. Privalov, J. Mol. Biol. 232 (1993) 639.
[16] P.L. Privalov, G.I. Makhatadze, J. Mol. Biol. 232 (1993) 660.
[17] G. Otting, K. Wüthrich, J. Am. Chem. Soc. 111 (1989) 1871.
[18] G. Otting, E. Liepinsh, Acc. Chem. Res. 28 (1995) 171.
[19] M.-C. Bellissent-Funel, J. Mol. Liq. 84 (2000) 39.
[20] G. Panick, R. Malessa, R. Winter, Biochemistry 38 (1999) 6512.
[21] J. Woenckhaus, R. Köhling, P. Thiyagarajan, K.C. Littrell, S. Seifert, C.A. Royer, R. Winter, Biophys. J. 80 (2001) 1518.
[22] G. Panick, R. Malessa, R. Winter, G. Rapp, K.J. Frye, C.A. Royer, J. Mol. Biol. 275 (1998) 389.
[23] J. Bandekar, Biochim. Biophy. Acta 1120 (1992) 123.
[24] M. Karas, F. Hillenkamp, Anal. Chem. 60 (1988) 2299.
[25] C.M. Whitehouse, R.N. Dreyer, M. Yamashuta, J.B. Fenn, Anal. Chem. 57 (1985) 675.
[26] R. Chen, X. Cheng, D.W. Mitchell, S.A. Hofstadler, Q. Wu, A.L. Rockwood, M.G. Sherman, R.D. Smith, Anal. Chem. 67 (1995) 1159.
[27] T.D. Wood, R.A. Chorush F.M. Wampler, D.P. Little, P.B. O'Connor, F.W. McLafferty, Proc. Natl. Acad. Sci. U.S.A. 92 (1995) 2451.
[28] F.W. McLafferty, Z. Guan, U. Haupts, T.D. Wood, N.L. Kelleher, J. Am. Chem. Soc. 120 (1998) 4732.
[29] S.-W. Lee, H.-N. Lee, H.S. Kim, J.L. Beauchamp, J. Am. Chem. Soc. 120 (1998) 5800.
[30] M. Dole, L.L. Mack, R.L. Hines, J. Chem. Phys. 49 (1968) 2240.

[31] C. Menzel, K. Dreisewerd, S. Berkenkamp, F. Hillenkamp, Int. J. Mass Spectrom. 207 (2001) 73.
[32] R.R. Hudgins, J. Woenckhaus, M.F. Jarrold, Int J. Mass Spectrom. Ion Processes 165/166 (1997) 497.
[33] R.D. Smith, K.J. Light-Wahl, B.E. Winger, J. Loo, Org. Mass Spectrom. 27 (1992) 811.
[34] M. Przybylski, O. Glockner, Angew. Chem. 108 (1996) 878; Angew. Chem. Int. Ed. Engl. 35 (1996) 806.
[35] S.J. Gaskal, J. Mass Spectrom. 32 (1997) 677.
[36] E.R. Williams, Anal. Chem. News Features 70 (1998) 179A.
[37] S.A. Lorenz, E.P. Maziarz III, T.D. Wood, Appl. Spectrosc. 53 (1999) 18A.
[38] D.B. Hagar, N.J. Dovichi, J. Klaasen, P. Kebarle, Anal. Chem. 66 (1994) 3944.
[39] R.D. Smith, K. Light-Wahl, J. Biol. Mass Spectrom. 22 (1993) 493.
[40] J. B. Fenn, J. Am. Chem. Soc. Mass Spectrom. 4 (1993) 524.
[41] B.A. Thomson, J.V. Iribarne, J. Chem. Phys. 71 (1979) 4451.
[42] J.V. Iribarne, B.A. Thomson, J. Chem. Phys. 64 (1976) 2287.
[43] F.W. Röllgen, F. Bramer-Wegen, L. Bütfering, J. Phys. (Paris), Colloq. 18 (1987) 243.
[44] G. Schmelzeisen-Redecker, L. Bütfering, F.W. Röllgen, Int. J. Mass Spectrom. Ion Processes 90 (1989) 139.
[45] J.N. Smith, R.L. Grimm, J.L. Beauchamp, J. Chem. Phys. (submitted).
[46] Transportproperties of Ions in Gases, E.A. Mason, E.W. McDaniel, (Eds.) Wiley, New York, 1988.
[47] Y. Kaneko, M.R. Megill, J.B. Hasted, J. Chem. Phys. 45 (1966) 3741.
[48] G.v. Helden, T. Wyttenbach, M.T. Bowers, Science 267 (1995) 1483.
[49] D.E. Clemmer, R.R. Hudgins, M.F. Jarrold, J. Am. Chem. Soc. 117 (1995) 10141.
[50] P. Dugourd, R.R. Hudgins, D.E. Clemmer, F.M. Jarrold, Rev. Sci. Instrum. 68 (1997) 1122.
[51] R.W. Purves, R. Guevrement, Rev. Sci. Instrum. 69 (1999) 4094.
[52] C.S. Hoaglund, S.J. Valentine, D.E. Clemmer, Anal. Chem. 69 (1997) 4156.
[53] M.F. Jarrold, E.C. Honea, J. Am. Chem. Soc. 114 (1992) 459.
[54] R. Diamond, D.C. Phillips, C.C. Blake, A.C.T. North, J. Mol. Biol. 82 (1974) 371.
[55] A. Wlodawer, J. Nachman, G.L. Gilliland, W, Gallagher, C. Woodward, J. Mol. Biol. 198 (1987) 469.
[56] G.W. Bushnell, G.V. Louie, G.D. Brayer, J. Mol. Biol. 214 (1990) 585.
[57] S.V. Evans, B.P. Sishta, A.G. Mauk, G.D. Brayer, Proc. Natl. Acad. Sci. U.S.A. 91 (1994) 4723.
[58] K.B. Shelimov, D.E. Clemmer, R.R. Hudgins, M.F. Jarrold, J. Am. Chem. Soc. 119 (1997) 2240.
[59] K.B. Shelimov, M.F. Jarrold, J. Am. Chem. Soc. 118 (1996) 10313.
[60] D.S. Gross, P.D. Schnier, S.E. Rodriguez-Cruz, C.K. Fagerquist, E.R. Williams, Proc. Natl. Acad. Sci. U.S.A. 93 (1996) 3143.
[61] T.D. Wood, R.A. Chrustii, F.M. Wampler, D.P. Little, P.B. O'Connor, F.W. McLafferty, Proc. Natl. Acad. Sci. U.S.A 92 (1995) 2451.
[62] M.F. Mesleh, J.M. Hunter, A.A. Shvartsburg, G.C. Schatz, M.F. Jarrold, J. Phys. Chem. 100 (1996) 16082.
[63] C. Wu, W.F. Siems, G.R. Asbury, H.H. Jr. Hill, Anal. Chem. 70 (1998) 4929.
[64] A.T. Iavarone, J.C. Jurchen, E.R. Williams, Anal. Chem. 73 (2001) 1455.
[65] Y. Mao, J. Woenckhaus, J. Kolafa, M.A. Ratner, M.F. Jarrold, J. Am. Chem. Soc. 121 (1999) 2712.
[66] S.J. Valentine, J.G. Anderson, A.D. Ellington, D.E. Clemmer, J. Phys. Chem. B 101 (1997) 3891.
[67] J. Woenckhaus, Y. Mao, M.F. Jarrold, J. Phys. Chem. B 101 (1997) 847.
[68] P.X. Qi, J.L. Urbauer, E.J. Fuentes, M.F. Leopold, A. Wand, J. Struct. Biol. 1 (1994) 378.
[69] Y.K. Lan, S. Ikuta, P. Kebarle, J. Am. Chem. Soc. 104 (1982) 1462.
[70] J.L. Fye, J. Woenckhaus, M.F. Jarrold, J. Am. Chem. Soc. 120 (1998) 1327.
[71] B. Lee, F.M. Richards, J. Mol. Biol. 55 (1971) 379.
[72] G.I. Makhataddze, P.L. Privalov, Adv. Prot. Chem. 47 (1995) 231.
[73] A. Ben-Naim, Biopolymers 29 (1990) 567.
[74] T. Lazaridis, G. Archontis, M. Karplus, Adv. Protein Chem. 47 (1995) 231.
[75] R.B. Sharma, P. Kebarle, J. Am. Chem. Soc. 106 (1984) 3913.
[76] M. Moet-Ner, L.W. Siek, S. Scheiner, X. Duan J. Am. Chem. Soc. 116 (1994) 7848.
[77] H. Thorell, Å. Åkesson, J. Am. Chem. Soc. 63 (1941) 1818.
[78] J. Woenckhaus, R.R. Hudgins, M.F. Jarrold, J. Am. Chem. Soc. 119 (1997) 9586.
[79] J.A. McCammon, B.R. Gelin, M. Karplus, Nature 267 (1977) 585.
[80] M. Levitt, R. Sharon, Proc. Natl. Acad. Sci. U.S.A. 85 (1988) 7557.
[81] J.A. Rupely, G. Careri, Adv. Protein Chem. 41 (1991) 37.
[82] A. Wlodawer, S. Waiter, R. Huber, L. Sjölin, J. Mol. Biol. 180 (1984) 301.
[83] A. Wlodawer, J. Nachman, G.L. Gilliland, W. Gallagher, C. Woodward, J. Mol. Biol. 198 (1987) 469.
[84] J. Deisenhofer, W. Steigemann, Acta Crystallogr. B. 31 (1975), 238.
[85] G. Otting, K. Wüthrich, J. Am. Chem. Soc. 111 (1989) 1871.
[86] J. Hermans, M. Vacatello, ACS Symp. Ser. 127 (1980) 199.
[87] Y. Mao, M.A. Ratner, M.F. Jarrold, Phys. Chem. B 103 (1999) 10017.
[88] J. Kolafa, unpublished (*http://www.icpf.cas.cz/jiri/*)
[89] B.R. Brooks, R.E. Bruccoleri, B.D. Olafson, D.J. States, S. Swaminathan, M. J. Karplus, J. Comput. Chem. 2 (1983) 187.
[90] W.F. Van Gunsteren, H. Berendsen, J.C. Mol. Phys. 34 (1977) 1311.
[91] Y. Mao, M.A. Ratner, M.F. Jarrold, J. Am. Chem. Soc. 122 (2000) 2950.
[92] S. Fischer, C.S. Verma, Proc. Natl. Acad. Sci. U.S.A. 96 (1999) 9613.
[93] H. Kamberaj, V. Helms, Phys. Rev. E (submitted).